TRANSGRANULAR AND INTERGRANULAR FRACTURE IN Al-Si-Mg CASTING ALLOYS

Q.G. Wang, C.H. Cáceres and J.R. Griffiths[a]

Co-operative Research Centre for Alloy and Solidification Technology (CAST)
Department of Mining, Minerals and Materials Engineering
The University of Queensland, Brisbane, Qld 4072, Australia

**CSIRO Division of Manufacturing Technology, P O Box 883,*
Kenmore, Queensland 4069, Australia

ABSTRACT

The fracture paths in broken tensile samples of commercial Al-7Si-Mg-T6 casting alloys have been determined. The results indicate that the fracture mode is predominantly intergranular for material with small dendrite arm spacing, but it becomes transgranular at large dendrite arm spacing, regardless of the Mg content. Modification with strontium shifts the transition in fracture mode to slightly larger dendrite arm spacing. The relationship between the fracture mode and tensile ductility of the alloys is discussed.

KEYWORDS

Fracture mode, aluminium, silicon, intergranular fracture, transgranular fracture.

INTRODUCTION

The failure of Al-7Si-Mg alloys is generally accepted to be the result of ductile fracture in three stages (Gurland and Plateau, 1963; Gangulee and Gurland, 1967; Frederick and Bailey, 1968; Singh and Flemings, 1969; Coade *et al.*, 1977; Meyers, 1987): (1) silicon particle cracking at very low plastic strains (1~2%); (2) growth of voids nucleated on the cracked Si particles by continued plastic strain, and (3) void and microcrack coalescence along the eutectic region by rupture of the aluminium matrix separating the voids. Frederick and Bailey (1968) observed that the fracture in casting Al-Si-Mg alloys occurs almost exclusively along dendrite cell boundaries and thus the fracture mode is predominantly transgranular. Here the term "grain" refers to a dendrite colony whilst "cell" refers to the dendrite arms. Voigt and Bye (1991) observed that the crack path in A356.0 alloys sometimes followed the grain boundaries but in general crack propagation occurred in a predominantly transgranular manner, following the cell boundaries. On the other hand, Fat-Halla (1987) found that fracture followed an intergranular path in rapidly solidified Sr-modified A356 alloy, while slowly solidified sand cast alloys showed a tendency towards transgranular fracture. Coade *et al.* (1977) reported an intergranular fracture mode for finer cell sizes in a Sr-modified Al-7%Si-0.4%Mg alloy. In a more recent study in a similar alloy, Cáceres *et al.* (1995) observed

that the fracture path is transgranular in large dendrite cell size material but becomes intergranular in small cell size material.

The present work was carried out to study the fracture mode in tensile samples with a variety of dendrite cell sizes and eutectic Si particle size and morphology. Different microstructures were produced by varying solidification rates while the particle morphology was changed by using chemical modification with Sr. Tensile samples deformed to fracture were anodised to reveal the grain structures. The relative proportions of fracture path along the cell and grain boundaries were determined.

EXPERIMENTAL PROCEDURE

Commercial unmodified Al-7%Si-0.4/0.66%Mg alloys (alloys AA601 and AA603, Australian nomenclature equivalent to the US A356.0 and A357.0, respectively) were used in this work. Modification was achieved by adding an Al-10%Sr master alloy to the unmodified melt just prior to degassing. The chemical compositions of the alloys are shown in Table 1. Casting plates were made in resin-bonded silica sand moulds with a large tapered chill at one end and a large riser at the other to produce quasi-directional solidification. The freezing rate varied from about 12°C/s near the chill to 0.2°C/s at the riser end (Cáceres *et al.*, 1995). The cast plates were sectioned into (15x15x50 mm^3) bars. The bars were hot isostatically pressed (HIP-ed) at 540°C and 100 MPa for 2 h to eliminate porosity. The HIP-ed bars were then solution treated at 540°C for 18 h, quenched in water at room-temperature, pre-aged at room temperature for 20 h and aged at 170°C for 6 h in a salt bath. The bars were then machined into flat tensile specimens of cross section 5×4 mm^2 and gauge length 15 mm. Tensile tests were conducted at 1 mm min^{-1}, and strains measured with an extensometer.

Table 1. Chemical analysis of the alloys [wt%].

Alloys	Si	Mg	Fe	Sr	Ti	Cr, Cu, Mn, Ni, Zn, Zr
Unmodified AA601	6.8	0.39	0.13	<0.001	0.13	<0.01
Sr-modified AA601	7.0	0.41	0.14	0.025	0.13	<0.01
Unmodified AA603	6.9	0.70	0.14	<0.001	0.09	<0.01
Sr-modified AA603	6.8	0.70	0.14	0.025	0.09	<0.01

In order to study the interaction between silicon particles and plastic flow during deformation, a number of tensile specimens had a face metallographically polished prior to deformation. After a predetermined deformation (usually between 1% and 3%), the samples were observed under the optical microscope using Nomarski interference contrast to reveal the slip bands.

The two halves of selected fractured tensile samples were mounted together after carefully matching the fracture surfaces, ground to remove about half the thickness and then polished to a fine SiO_2 finish. Subsequently, the samples were anodised at 30V for 30 seconds in a 2% solution of fluoroboric acid to reveal the grain structure. The anodised samples were then observed on an optical microscope under polarised light to reveal the grains. The grain size was measured by linear intercept and the relative proportion of intergranular/transgranular fracture was determined by measuring the length of the fracture path along the grain boundaries and across the grains. The results were expressed as the ratio between the length of the intergranular portion and the total length of fracture path across the studied sample. A number of samples were also deep-etched in a solution (5%) of perchloric acid in ethanol at

10 V & 0.3 A for 20 min to reveal the eutectic structure and then observed on a scanning electron microscope.

Quantitative metallography was carried out using a Quantimet image analyser (Cambridge Instrument, Model 570). The as-cast dendrite arm spacing (DAS) was measured in samples obtained from different locations in the cast plates.

RESULTS AND DISCUSSION

Typical results after anodising the samples are shown in Figs. 1 and 2, for unmodified and Sr-modified alloys. Inspection of the anodised samples indicated that for large cell size material fracture tends to occur along the dendritic cell boundaries, while for smaller cell size material the fracture path runs along grain boundaries in an increasing proportion.

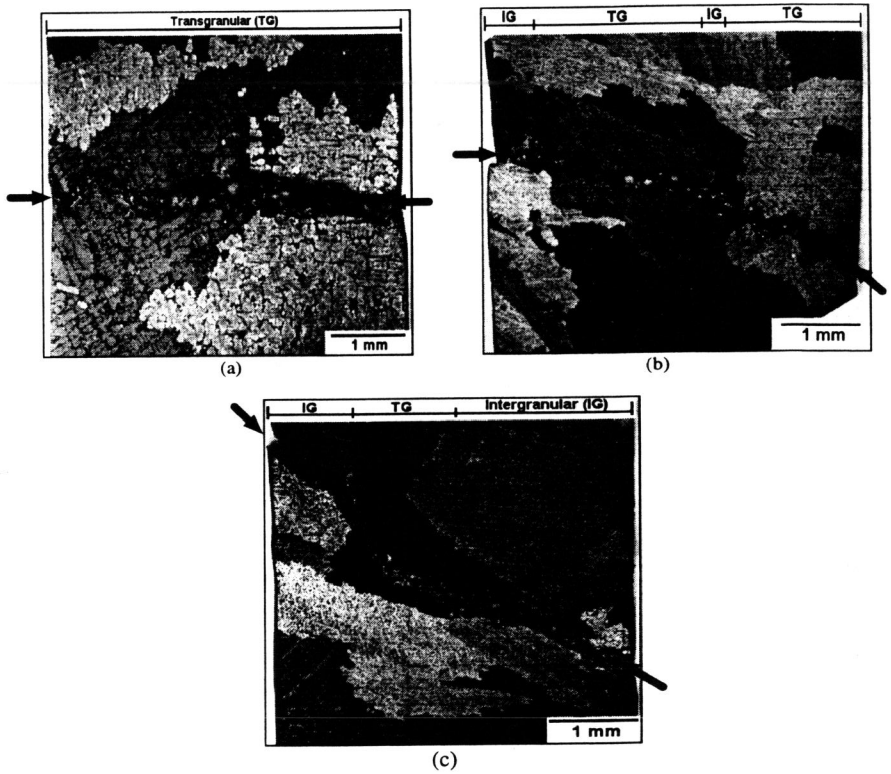

Fig. 1. Anodised longitudinal sections of fractured samples showing the grain structure and the fracture path (identified by the arrows). The figures in square brackets indicate the proportion of intergranular fracture. (a) DAS: 52 μm [0%], (b) DAS: 27 μm [19%], and (c) DAS: 25 μm [57%]. Unmodified alloy. TG denotes transgranular, IG denotes intergranular.

The proportion of intergranular fracture is shown in Figs. 3 and 4 as a function of the DAS, together with the elongation to fracture. Plotted values are the average of 2 or 3 samples. It can be seen that the proportion of intergranular fracture increases from zero for large DAS values to about 60% for small DAS. It can also be seen that the ductility increases as the fracture mode changes from transgranular to intergranular. For the Sr-modified alloys the transition in the fracture mode takes place at a larger DAS than with the unmodified alloys. The Mg content does not affect the DAS at which the transition takes place.

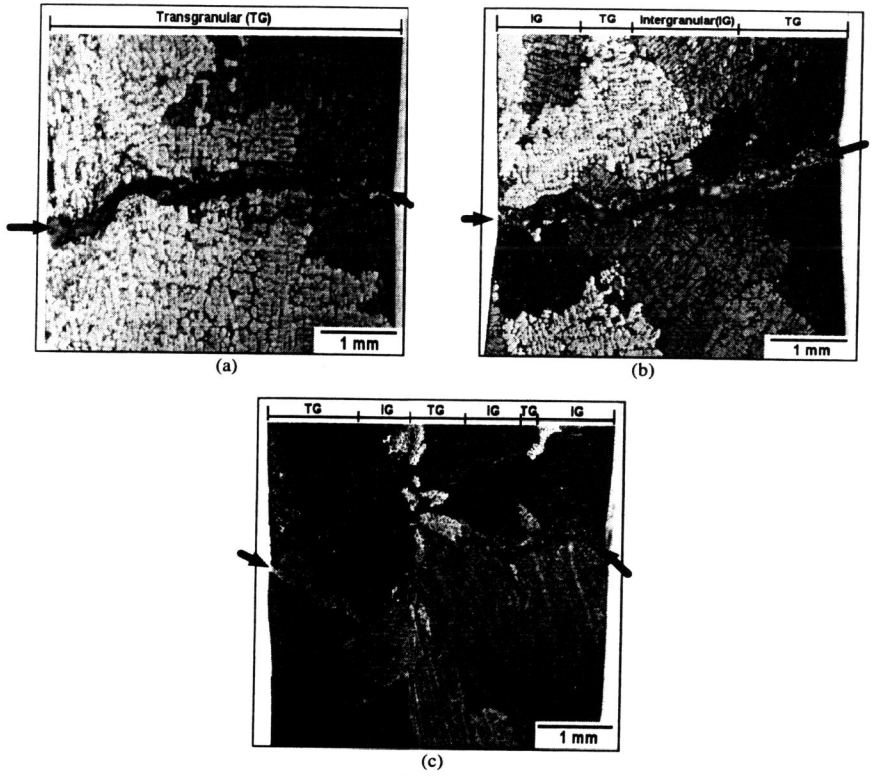

Fig. 2. Anodised longitudinal sections of fractured samples showing grain structure and the fracture path (identified by the arrows). The figures in square brackets indicate the proportion of intergranular fracture. (a) DAS: 52 μm [0%], (b) DAS: 45 μm [51%], and (c) DAS: 25 μm [58%]. Sr-modified alloy. TG denotes transgranular, IG denotes intergranular.

The mean grain size was independent of composition and varied from ~0.8 mm (for the fastest cooling rate) to ~1.2 mm (for the slowest cooling rate), although, as Fig. 1 shows, much larger grains were common. This small effect of cooling rate on grain size is to be expected for alloys which contain a grain refiner (Apelian and Chen, 1986).

Figures 5 and 6 show the structure of the dendritic cell boundaries after deep-etching the matrix (unmodified alloy). Figure 5 shows that for large DAS, both cell and grain boundaries are very distinct, while for small DAS, Fig. 6, the small and widely spaced Si particles barely define the cell boundaries. The structure of the dendrite cell boundaries determines the degree of interaction between the plastic deformation and the cell boundaries. This is made evident by the Nomarski interference contrast micrographs of Figs. 7 and 8 where the interaction between the slip bands and the dendrite cell boundaries and grain boundaries is shown. In the coarser structures (Fig. 7), the cell boundaries form effective obstacles to slip. In contrast, in the finer structures (Fig. 8) the cell structure is less distinct (as noted in Fig. 6) and the particles interact with the slip bands individually rather than collectively as in the case of Fig. 7. This leads to a strong interaction between slip bands and grain boundaries, as illustrated also by Fig. 8. These observations confirm conclusions made on the basis of observations on the polished surface of tensile samples (Cáceres *et al.*, 1995).

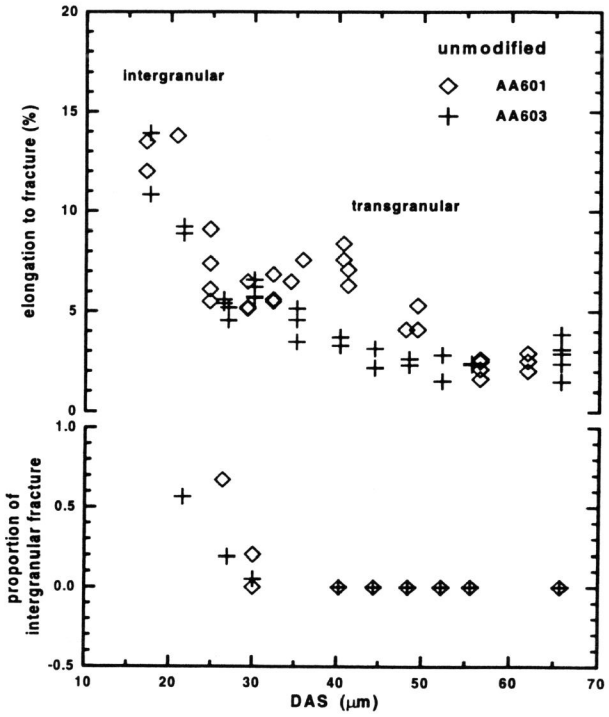

Fig. 3. The proportion of intergranular fracture and the tensile ductility as a function of the dendrite arm spacing. Unmodified alloys.

The differences in the interaction of the slip bands with the cell and grain boundaries have consequences for the distribution of cracked silicon particles during plastic straining, both for unmodified or Sr-modified alloy. In material with large DAS and therefore distinct cell boundaries, the cracked particles are found preferentially in the cell boundaries while in material with small DAS the cracked particles are preferentially located in the grain boundaries. This determines whether the final fracture will tend to occur along either the grain or the cell boundaries (Wang and Cáceres, 1996).

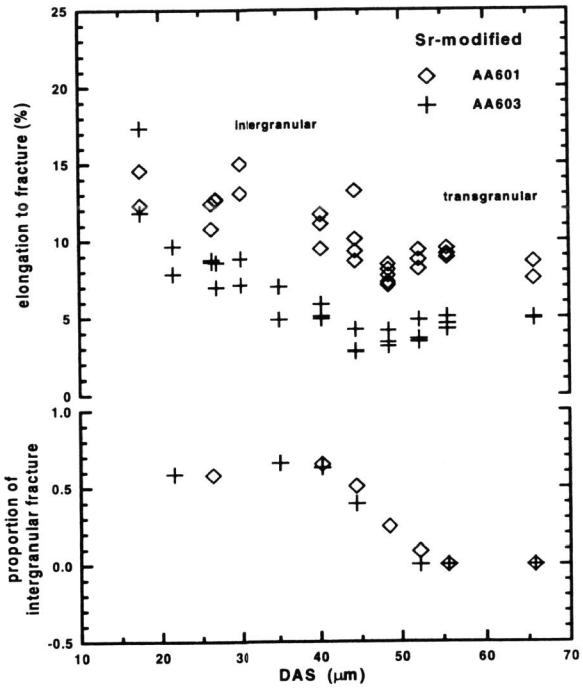

Fig. 4: The proportion of intergranular fracture and the tensile ductility as a function of the dendrite arm spacing. Sr-modified alloys.

It is known that particle cracking in these alloys starts at low plastic strains, about 1-2% (Gangulee and Gurland, 1967; Frederick and Bailey, 1968; Coade *et al.*, 1977; Cáceres *et al.*, 1995). As the applied strain increases, localised shear bands form at the tips of the cracked particles and these bands eventually lead to void coalescence and final fracture. Coarser structures with well defined cell boundaries provide an easy path for the percolation of damage across the sample (Cáceres *et al.*, 1995), leading to a predominantly transgranular fracture. In the finer structures, on the other hand, the preferential damage along grain boundaries leads to intergranular fracture. It is noteworthy that the intergranular fractures are those with the highest

ductility. The same pattern of behaviour is observed in both unmodified and strontium-modified alloy. Thus, a conclusion can be made that the high elongations observed for smaller cell sizes are associated with the disappearance of the cell boundaries during solution-treatment which leads to an intergranular fracture mechanism. The coarser cells have boundaries which can block slip bands even after heat treatment; such microstructures are prone to fail by a less ductile, transgranular fracture mode.

Fig. 5. Deep-etched sample showing the structure of the dendritic cell boundaries in a sample with large cell size. DAS: 40 μm. Unmodified alloy.

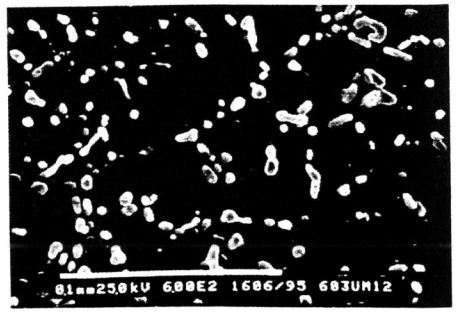

Fig. 6. Deep-etched sample showing the structure of the dendritic cell boundaries in a sample with small cell size. DAS: 17 μm. Unmodified alloy.

50 μm

Fig. 7. Nomarski-contrast micrograph showing the interaction between slip bands and Si particles in cell boundaries in a sample with large cell size. DAS: 56 μm. Applied strain: 1.4%.

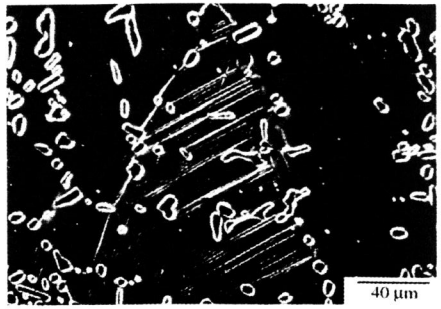

Fig. 8. Nomarski-contrast micrograph showing the interaction between slip bands and Si particles in grain boundaries in a sample with small cell size. DAS: 27 μm. Applied strain: 3.1%.

CONCLUSIONS

The fracture path in material with large dendrite cell sizes is predominantly transgranular, the final fracture occurring along the cell boundaries. In material with small dendrite cell size the fracture mode tends to be intergranular. This behaviour is not affected by the Mg content. Modification with Sr shifts the transition in fracture mode towards larger values of the dendrite cell size.

The transition from transgranular to intergranular fracture mode is accompanied by an increase in the ductility of the alloys.

REFERENCES

Apelian, D. and J.J.A. Chen (1986). *Trans. Amer. Foundrymen's Soc.*, 94, 797.
Cáceres, C.H., C.J. Davidson and J.R. Griffiths (1995). *Materials Science and Engineering*, A197, 171.
Coade, R. W., S. M. Nugent, D. S. Saunders, J. R. Griffiths and B. A. Parker (1977). *Proc. Annual Conf. Aust. Inst. Metals,* Australian Inst. of Metals, Melbourne, 6B-1.
Fat-Halla, N. (1987). *Journal of Materials Science,* 22, 1013.
Frederick, S. F. and W. A. Bailey (1968). *Trans. Metall. Soc. AIME*, 242, 2063.
Gangulee, A. and J. Gurland (1967). *Trans. Metall. Soc. AIME,* 239, 269.
Gurland, J. and J. Plateau (1963). *Trans. Metall. Soc. AIME*, 5, 442.
Meyers, C. W. (1986). *Trans. Amer. Foundrymen's Soc.*, 94, 511.
Singh, S.N. and M.C. Flemings (1969). *Trans. Metall. Soc. AIME*, 245, 1181.
Voigt, R.C. and D.R. Bye (1991). *Trans. Amer. Foundrymen's Soc.*, 99, 33.
Wang, Q.G. and C.H. Cáceres (1996). *Proc. 4th Asian Foundry Conf.*, Australian Foundry Inst, Brisbane.